Ultrahigh vacuum/high-pressure flow reactor for surface x-ray diffraction and grazing incidence small angle x-ray scattering studies close to conditions for industrial catalysis

R. van Rijn, M. D. Ackermann, O. Balmes, T. Dufrane, A. Geluk, H. Gonzalez, H. Isern, E. de Kuyper, L. Petit, V. A. Sole, D. Wermeille, R. Felici, and J. W. M. Frenken

Citation: Review of Scientific Instruments **81**, 014101 (2010); doi: 10.1063/1.3290420

View online: http://dx.doi.org/10.1063/1.3290420

View Table of Contents: http://aip.scitation.org/toc/rsi/81/1

Published by the American Institute of Physics

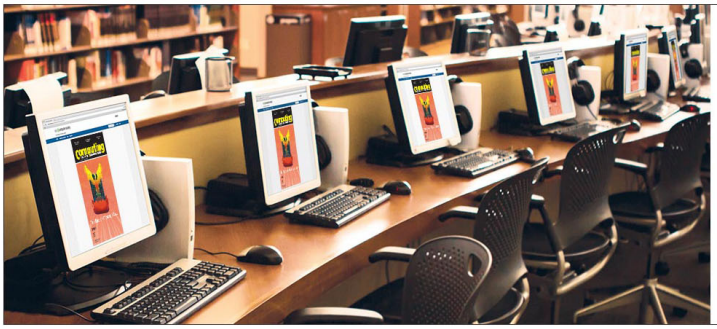

Ultrahigh vacuum/high-pressure flow reactor for surface x-ray diffraction and grazing incidence small angle x-ray scattering studies close to conditions for industrial catalysis

R. van Rijn,[1,2] M. D. Ackermann,[1,2] O. Balmes,[2] T. Dufrane,[2] A. Geluk,[1] H. Gonzalez,[2] H. Isern,[2] E. de Kuyper,[1] L. Petit,[2] V. A. Sole,[2] D. Wermeille,[2] R. Felici,[2] and J. W. M. Frenken[1]
[1]*Kamerlingh Onnes Laboratory, Leiden University, P.O. Box 9504, RA Leiden 2300, The Netherlands*
[2]*European Synchrotron Radiation Facility, B.P. 220, Grenoble F-38043, France*

(Received 4 November 2009; accepted 16 December 2009; published online 25 January 2010)

A versatile instrument for the *in situ* study of catalyst surfaces by surface x-ray diffraction and grazing incidence small angle x-ray scattering in a 13 ml flow reactor combined with reaction product analysis by mass spectrometry has been developed. The instrument bridges the so-called "pressure gap" and "materials gap" at the same time, within one experimental setup. It allows for the preparation and study of catalytically active single crystal surfaces and is also equipped with an evaporator for the deposition of thin, pure metal films, necessary for the formation of small metal particles on oxide supports. Reactions can be studied in flow mode and batch mode in a pressure range of 100–1200 mbar and temperatures up to 950 K. The setup provides a unique combination of sample preparation, characterization, and *in situ* experiments where the structure and reactivity of both single crystals and supported nanoparticles can be simultaneously determined.
 [doi:10.1063/1.3290420]

I. INTRODUCTION

Until the late 1990s, direct experimental evidence on the working mechanisms of heterogeneous catalysis at the molecular level was largely based on surface-science studies under ultrahigh vacuum (UHV) and high-vacuum conditions ($<10^{-5}$ mbar). UHV conditions provide electrons and ions long mean free paths compared to ambient pressure conditions, allowing one to use electron-based and ion-based techniques, such as low energy electron diffraction and low energy ion scattering. This approach has been very successful in acquiring understanding of the fundamental interaction of molecules with single-crystalline surfaces for a large variety of catalytic systems.[1,2]

In industrial catalysis however, the vast majority of interaction processes of molecules with a surface happen at elevated temperatures and at high pressures (>1 bar). This discrepancy is known as the pressure gap.[3] Furthermore, a catalyst is usually not a macroscopic, low-index, single-crystal surface but very often it consists of oxide-supported nanometer size particles. Hence structural and electronic particle size effects and particle-support interactions likely influence the catalyst.[4] This last discrepancy is called the materials gap. There is a growing body of evidence that one can often not simply extrapolate UHV results to atmospheric pressures. The structure and morphology of the catalyst surface at realistically high pressures and temperatures may differ significantly from the situation at low pressures (and temperatures), which can lead to dramatic differences in reaction mechanism and catalytic performance (efficiency and selectivity). Recently a growing number of surface-science techniques, traditionally developed for UHV, are being adapted to operate under "realistic" reaction conditions.[5] Notable examples of this development are high-pressure transmission electron microscopy,[6] high-pressure scanning tunneling microscopy (ReactorSTM),[7,8] high-pressure x-ray photoelectron spectroscopy,[9] and high-pressure surface x-ray diffraction (SXRD).[10,11]

The weak interaction of x-rays with low-electron-density materials (gasses) makes x-ray-based techniques suitable for studying catalyst at realistic conditions. This is reflected in the large number of x-ray absorption fine structure (XAFS) and powder diffraction studies of catalysts. For studying catalytically active *surfaces* under realistic conditions, SXRD (Refs. 12 and 13) and grazing incidence small angle x-ray scattering (GISAXS) (Ref. 14) are extremely suitable. It can be called surprising that only a handful of setups suitable for this type of research exist. The typical geometry for a SXRD-type reactor is a vessel with transparent walls for x-rays (e.g., beryllium, aluminum) in which one can introduce gas mixtures of different compositions. UHV is often required for proper sample preparation, so these vessels are often quite big (>1 liter) and can, apart from being used at high gas pressures, also be evacuated to pressures below 10^{-9} mbar. Another method frequently implemented is a UHV sample transfer from a preparation setup to the reactor setup. All these designs have the major disadvantage that the reactors are operated in batch mode, which implies that the gas composition in the reactor changes over the course of a measurement. Nevertheless excellent results have been obtained in batch reactors.[15–18] A second disadvantage of the transfer method is the necessary realignment of the sample with respect to the x-ray beam in diffraction experiments after each transfer.

In this paper we introduce a novel reactor setup for use in conjunction with a six-circle diffractometer for SXRD/GISAXS experiments. It has been developed within the framework of a collaboration between the Interface Physics Group at Leiden University and the beamline staff at ID03, the surface diffraction beamline of the European Synchrotron Radiation Facility. The instrument bridges both the pressure gap and the materials gap without introducing the two disadvantages mentioned above (batch and realignment). It combines a small volume flow reactor with sample preparation under UHV conditions. Furthermore it enables us to determine surface structure and morphology under reaction conditions by SXRD or GISAXS and simultaneously measure the reaction kinetics by mass spectrometry. Examples of reactions we would like to study are: CO oxidation on Pt-group metals [both single crystals and nanoparticles (NPs)],[1–3] NO reduction in Pt-group metals,[19] ethylene epoxidation on Ag nanoparticles,[20] partial methane oxidation,[21] desulphurization,[22] and the Fischer Tropsch reaction.[23] We start by describing the requirements for such a setup and introduce the general architecture of the instrument. The paper ends with a demonstration of the performance of the instrument during CO oxidation experiments on Pd(111) and Pd(100).

II. DESIGN SPECIFICATIONS

The combination of several sample preparation techniques typically requires an UHV chamber with a relatively large (>1 liter) volume. For the preparation of both single-crystal surfaces and oxide-supported NPs, the instrument has to combine facilities for ion bombardment, vacuum deposition, and vacuum annealing. To guarantee sample cleanliness this preparation should be performed *in situ*, without transport through the atmosphere prior to experiments. Characterization of the sample at intermediate stages of preparation under UHV conditions should be possible with x-rays.

For experiments under catalytic conditions the requirements are different. The gas pressure around the sample needs to increase to the atmospheric pressure regime, while the gas composition in the reactor is determined by mass spectrometry simultaneously with the SXRD/GISAXS measurement. This experimental approach allows one to correlate reaction kinetics with surface structure and morphology.

Furthermore the partial pressures of the reactant gasses should be fully controllable and it should be possible to keep them constant in time. This is necessary in order to map out the precise behavior of a model catalyst as a function of gas composition or as a function of time under constant gas and temperature conditions. This implies that the instrument should have the character of a flow reactor, rather than a batch reactor, in which the gas conditions would be changing continually. The characteristic refresh time of the reactor is determined by the reactor-volume-to-gasflow ratio, whereas the chemical resolution in the gas detection is determined by the sample-surface-to-gasflow ratio. For a given sample size and chemical resolution one would thus like to make the volume of the reactor small. This requirement obviously conflicts with the relatively large volume that is required for the sample preparation.

The reactor wall material needs to be a low Z material, e.g., beryllium, aluminum, or Kapton®, to allow the x-rays to pass through. When the reactor is closed, no part of the setup, except for the beryllium window, is allowed to exceed the height of the sample, guaranteeing access to the full 2π hemisphere of incoming and diffracted photons. Since the setup is intended to be used for synchrotron-based SXRD and GISAXS experiments, it should be designed to fit and move on a six-circle diffractometer. To make optimal use of expensive synchrotron beamtime a quick sample exchange mechanism is also required.

III. DESIGN

In this section, we discuss the general architecture of the new setup, the design of its individual components, and the underlying considerations for specific design choices.

A. UHV chamber

The combination of all the mentioned requirements suggests a setup which combines two compartments with a transport mechanism in between: a reactor part and an UHV part. Typically one would transport the sample after preparation from UHV to the reactor. For the XRD experiments this would mean that one would have to realign the sample after every preparation cycle. For experiments at a synchrotron, this would imply an additional loss of valuable beamtime with every preparation cycle, a very undesirable situation. Instead of using a sample transfer mechanism we chose to keep the sample fixed inside the setup and to move the upper part of the setup around the sample. The design of the novel flow setup is shown in Fig. 1. The chamber consist of two steel plates connect by a bellow. The lower plate is mounted on a five-axis positioning system that is part of a six-circle diffractometer.[24] The lower plate holds the sample holder, the quadrupole mass spectrometer (QMS), and the turbopump. The top plate holds the ion gun and evaporator and can be translated vertically. If the bellow is completely extended as shown in Fig. 1(a), the setup is in the sample preparation configuration, in which the sample can be sputtered, annealed, and metal can be deposited on the sample. After preparation, the top part of the chamber can be lowered over the sample, as shown in Fig. 1(b). This is achieved by compressing the bellow between the top and bottom plates by means of a chain drive mechanism, until the top flange lands on the sample holder support. In the latter geometry, the small volume around the sample is fully separated from the UHV in the remainder of the system, which consists of the compressed bellow and the sample preparation tools. The upper part of this small reactor volume is defined by a beryllium dome[25–27] with good transparency for the x-rays. The reactor walls (top flange and dome) are actively cooled by a water flow through the top flange as shown in Fig. 1(a). This is done to prevent reactant gasses from reacting on and/or with the reactor walls at high temperatures. Both effects are highly undesirable.

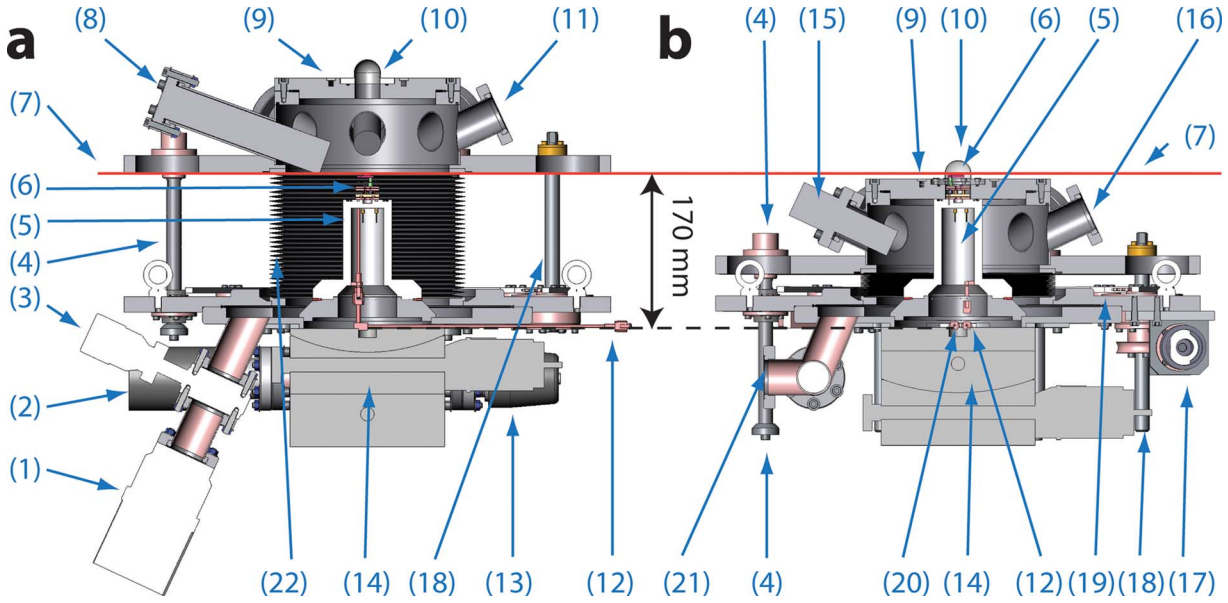

FIG. 1. (Color online) (a) Cut view of the setup in the UHV sample preparation geometry. (b) Cut view of the setup with closed reactor, 90° rotated with respect to the view of Fig. 1(a). The beam is located 170 mm above the diffractometer sample stage surface. The labels denote: (1) turbo pump, (2) quadrupole mass spectrometer, (3) manual UHV valve, (4) guiding rods for vertical movement of top part of the chamber, (5) sample holder foot, (6) sample holder, (7) x-ray beam height, (8) evaporator port, (9) water-cooled top flange, (10) 180° × 360° beryllium dome, (11) ion gun port, (12) reactor gas exhaust line, (13) UHV leak valve, (14) Huber five-axis positioning system, (15) cold cathode pressure gauge, (16) blind flange, (17) electromotor and drive shaft, (18) threaded drive rods for vertical movement of top part of the chamber, (19) chain drive mechanism for vertical movement, (20) gas entry line, (21) UHV vent valve, and (22) steel bellow.

The top flange seals the reactor from the UHV by a so-called V-seal®, that is normally intended for use in jet engines, cryogenic applications, etc.[28] The V-seals® are made of a gold coated nickel alloy, they seal UHV tight ($<10^{-10}$ mbar l/s He) and are reusable up to 30 times. The gold coating protects the seal from the reactants and guarantees its inertness. We prefer these V-seals over traditional elastomer seals, as the latter ones can only be used up to typically 500 K and they contain materials that might either influence the reaction or be influenced by the reactants.

Gasses are mixed in a gas system and transported to and from the reactor by two capillaries coming from under the sample holder support. Gas analysis was designed to be performed by dosing gas from the reactor exhaust pipe via a leak valve into the UHV part of the chamber, which is equipped with a QMS. When the sample is in UHV the gas lines are closed with two Swagelok® manual valves. The sample mounting plane of the standard sample holder is situated 4 mm above the top flange. The setup is currently equipped with the following UHV components:

- Varian[29] V-81-M turbomolecular pump with a pumping speed of 50 l/s for N_2 and a compression ratio of 5×10^8.
- Omicron[30] EFM3 evaporator mounted under a 20° angle relative to the sample horizon.
- SPECS[31] IQE 11/35 ion gun mounted under a 25° angle relative to the sample horizon.
- Cold cathode pressure gauge (Arun Microelectronics Ltd[32]).
- MKS Instruments[33] Micro Vision Plus QMS.
- Pfeiffer[34] All Metal regulating Valve UDV 146. This valve is used for backfilling the chamber for ion bombardment of the sample.
- Beryllium[25] dome with a radius of 14 mm and a wall thickness of 0.4 mm, or an aluminum dome with the same radius and a wall thickness of 1 mm.

Both the evaporator and the ion gun were slightly modified to minimize the blocking of the x-ray beam due to parts of these devices that would otherwise protrude above the sample surface.

B. Sample holder

Figure 2(a) shows a cut view of the top part of the system, with the top flange in its lower position, so that the sample holder is fully enclosed by the reactor part of the setup. The x-ray beam height is shown in red. The sample holder is shown in Fig. 2(b). It is easily removable from the sample support, by unscrewing the Be dome and pulling the holder out of the electrical connections, thus enabling rapid sample exchange (see below).

The materials that make up both the reactor and the sample holder have been chosen carefully not to be catalytically active. They all can withstand both oxygen and hydrogen at a pressure of 1 bar and a sample temperature of 950 K. The sample is heated by a graphite heating element embedded in boron nitride,[35] which is electrically and mechanically connected by two tungsten rods. These rods are clamped with stainless steel clamps from underneath the holder. Further electrical connection to the outside is made by two male/female connections and a feedthrough. The temperature of the sample is measured by a type C thermocouple (tungsten 95% rhenium 5%—tungsten 74% rhenium 26%). Note, that thermocouples containing Cu, Pt or Ni cannot be used. Pt is a highly active catalyst for CO oxidation, Ni forms carbonyls

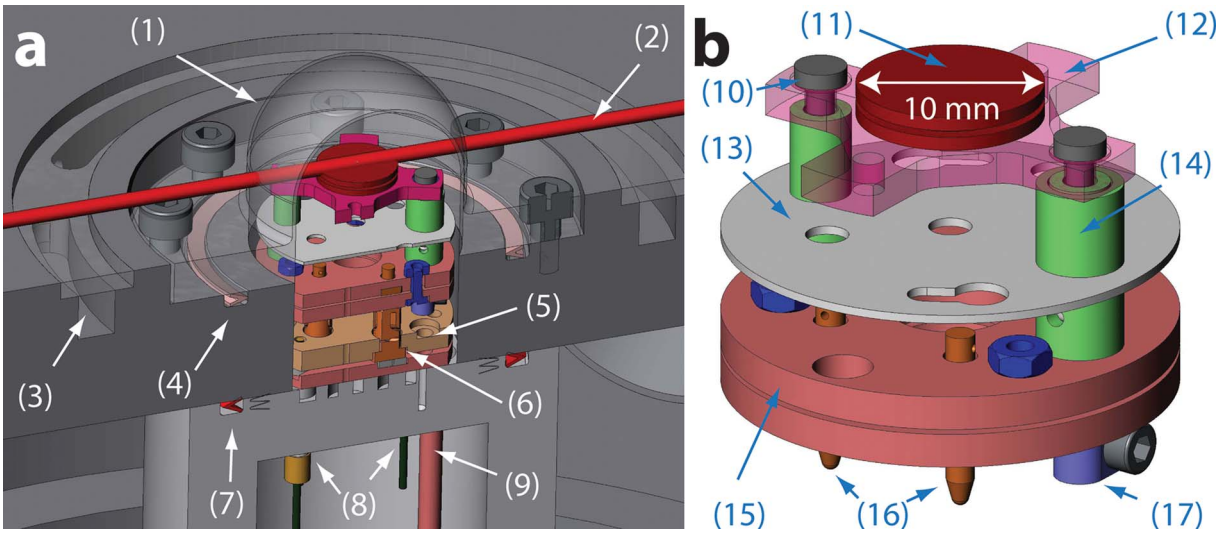

FIG. 2. (Color online) (a) Top part of the setup with the top flange in the lower position and with the sample holder in the reactor part of the system. (b) Sample holder. The labels denote: (1) beryllium dome, (2) x-ray beam height, (3) water cooling channel, (4) V-seal between the reactor and the external atmosphere, (5) alumina plate, (6) female electrical connection, (7) V-seal between UHV and high pressure in the reactor, (8) electrical feedthroughs, (9) gas entry line, (10) tungsten rod, (11) sample, (12) boralectric heater, (13) heat shield, (14) alumina cylinder, (15) alumina plates, (16) male electrical connections, and (17) stainless steel clamps.

with CO, resulting in Ni deposition on the sample, and Cu is an active catalyst for methanol synthesis. The thermocouple is either spot-welded to, or pressed against the sample by two clips mounted on the heater (not shown in the figure). Unfortunately, feedthroughs are not available in thermocouple material (W, Re). Feedthroughs do exist of compensation material, equivalent to a type C thermocouple. However, these contain Ni and Cu, which cannot be tolerated. Therefore, we have chosen to equip the sample holder support with stainless steels feedthroughs and calibrate the temperature drop over the feedthroughs under various operating conditions of the reactor.

The exposed hot parts of the heater are protected from oxidation by a layer of boron nitride (BN) coating (COMBAT® Boron Nitride Coatings).[36] The sample fixation is chosen on a per-experiment basis. Usually Ta clips are used in oxidizing conditions and Mo clips in hydrogen-rich conditions. Ta is more resistant to oxidation than Mo but will eventually also oxidize at high temperatures. Ta, however, forms hydrides in hydrogen-rich conditions, whereas Mo does not.

C. Gas system

Figure 3 shows a schematic drawing of the gas system. It consists of four mass flow controllers (Bronkhorst[37] EL-FLOW, 50 ml_n/min) calibrated for different gasses. The common output is connected to the reactor via a flexible UHV-compatible polyether ether ketone (PEEK) tube (Sigma Aldrich,[38] 1.57 mm inner diameter). A pressure controller (Bronkhorst[37] EL-PRESS, 1200 mbar) is mounted on the reactor exhaust. This geometry allows us to independently set the reactor pressure, the gas composition, and the total mass flow. The pressure difference that is required to obtain a continuous flow of gas between the outlet of the mass flow controllers and the inlet of the pressure controller is determined by Poiseuille's law, approximated for an isothermal ideal gas

$$\Phi = \frac{\pi D^4}{256\eta L}\left(\frac{P_i^2 - P_o^2}{P_o}\right), \tag{1}$$

where Φ is the volumetric flow rate, D is the pipe diameter, η is the dynamic viscosity of the gas, L is the length of the pipe, and P_i and P_o are the inlet and outlet pressures, respectively. In Fig. 3 the flow resistance between the mass flow controllers and the pressure controller is determined by the PEEK tube and the stainless steel piping to and from the reactor. The pressure difference between the mass flow controllers and the pressure controllers that is needed to maintain a 50 ml_n/min (1 ml_n is defined as 1 ml at a gas temperature of 0 °C and a pressure of 1013 bar) flow of air

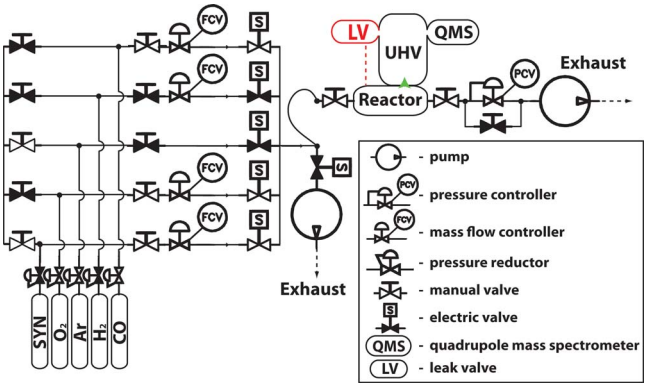

FIG. 3. (Color online) Schematic drawing of the gas system. Black valves are closed, white valves are open. In this typical configuration CO and O_2 are flowing through their respective controllers, while argon is bypassing on the left side via the lower controller. The final mixture flows through the reactor and is pumped away by the exhaust system via a pressure controller and a scroll pump. The gas composition in the reactor is analyzed by mass spectrometry. Initially a bypass line with a leak valve was designed to admit gas from the reactor to the UHV system with the mass spectrometer, but in practice we make use of a direct, tunable leak at the seal between the reactor and the UHV, symbolized here by the arrowhead between the reactor and the UHV. A carbonyl trap is mounted optionally between the CO bottle and the CO mass flow controller.

through the reactor is calculated to be 10 mbar. This makes that the pressure as measured at the pressure controller is nearly equal to the gas pressure in the reactor.

The pressure controller can regulate the total pressure in the reactor from 100 up to 1200 mbar. The flow controller can regulate the flow from 1 up to 50 ml_n/min. In a binary mixture of pure gasses at a total flow of 50 ml_n/min, the lowest composition of one of the gasses in the mixture is 2%. That would for example be 1 ml_n/min of gas A mixed with 49 ml_n/min of gas B. Therefore the lowest attainable partial pressure of this gas in the reactor is 2 mbar (2% of the minimum total pressure). If necessary this value can be lowered further by using bottles which contain mixtures of gas A and gas B.

The mass flow controllers, pressure controllers, the electric valves, and also the heater power supply are interfaced with SPEC, the beamline data acquisition software package.[39] This enables us to perform fully automated scanning of gas and temperature conditions and to use measurement macros with complex variations in time of all parameters, including abrupt switching of gas conditions. All these manipulations are possible during x-ray scattering experiments, without the need to interrupt the x-ray beam. Compared to the manual gas handling on the previous batch reactor,[10] this is a major improvement.

For many reactions, the catalytic conversion rate is determined by measuring the partial pressure of the reaction product by use of the QMS, in combination with accurate knowledge of the total pressure and flow in the reactor. Occasionally, however, the reaction rate will be so low that the partial pressure of the product gas is below the detection limit or below the background partial pressure of this gas in the QMS. If this is the case, the flow can be interrupted to make the reactor behave as a small batch reactor. One can then wait sufficiently long to see the partial pressure of the product increase and determine the chemical conversion rate from the rate of this increase.

IV. PERFORMANCE

The setup has been successfully tested in a number of experiments already. The results of these experiments will be published elsewhere. Here, we briefly describe the performance of several key aspects of the design and provide one example of the performance during an experiment.

A. UHV chamber

The UHV chamber reaches a base pressure of 4×10^{-9} mbar routinely after each bake out (120 °C × 24 h) against the turbomolecular pump. During reactivity measurements the temperature of the reactor wall does not exceed 333 K while the sample is at 875 K due to the efficient water cooling on the reactor walls.

The part of the gas system that was designed to admit gas from the reactor exhaust into the UHV chamber via a leak valve was never implemented. Instead, we tune the electromotor that drives the top flange of the setup. With this, we can regulate the leak via the V-seal® into the UHV, such as in a leak valve. The chamber pressure can be accurately set between 10^{-9} and 10^{-3} mbar. The small leak allows for the analysis of the gas composition in the reactor with the QMS mounted in the UHV part of the chamber. A leak directly at the reactor is advantageous because it does not introduce additional time delays or convolution effects in the detected gas composition.

B. Sample holder

With the top flange in the lower position, samples can be exchanged very quickly, e.g., within 30 min, effectively using the reactor as a load lock. In this way costly synchrotron time can be used efficiently. The base pressure for UHV sample preparation after changing sample is usually increased from 10^{-9} to 10^{-8} mbar because the reactor and the gas lines cannot be baked out separately.

A systematic error in the temperature reading of the thermocouple is made because of the temperature difference over the stainless steel feedthroughs. This systematic error was measured and carefully calibrated, resulting in a thermocouple temperature measurement accurate to within 3 K, by eliminating the systematic error.

Under UHV conditions the sample can be heated reliably up to 1500 K. In oxidizing conditions with Ta clips the sample can be heated to 950 K. Preliminary tests in which the sample was fixed to the heater by a BN coating show that the sample can reach a temperature of 1100 K in oxidizing reaction conditions. In this test the heat shield had to be removed from the sample holder as it was significantly catalyzing the oxidation of methane.

C. Gas system

The lower limit of the time constant of gas composition changes in the reactor at a constant operating pressure and a constant total mass flow is given by

$$\tau = \frac{VP_r}{F}, \tag{2}$$

where V is the reactor volume, P_r is the pressure in the reactor, and F is the total mass flow through the reactor. The time constant may be longer if there are dead volumes in the reactor or the gas lines or if the gas line diameters are such that the gas in the reactor diffuses into the gas inlet and gas outlet. The reactor volume as drawn in Fig. 2 is calculated to be 13.3 ml. Figure 4 shows a decaying partial argon pressure with a time constant of 15.8 s. On the basis of the calculated reactor volume one would expect a time constant of 12.4 s at the specified total mass flow and total pressure. We ascribe the 3.4 s difference in measured and calculated time constant to the fact that the gas in the reactor is not perfectly mixed within the characteristic refresh time. That means that part of the volume of the reactor is effectively "dead," i.e., it is refreshed mainly by gas diffusion rather than flow or convection. The diffusion of reactor gas into the gas line is negligible, as the flow speed in the gas lines is higher than the diffusion rates of the gasses.

Similarly, the rate at which the total pressure in the reactor can change at constant flow is given by the ratio of the total mass flow and the total gas system volume, i.e., the

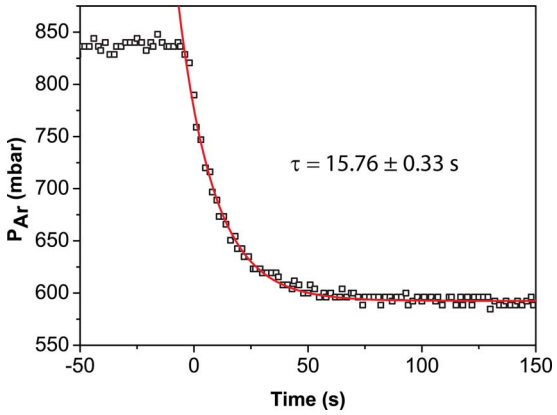

FIG. 4. (Color online) Exponential decay of the partial Ar pressure in the reactor measured by the QMS after switching the gas flow from a total rate of 64.8 ml_n/min with 84.8% Ar to a flow of 59.8 ml_n/min containing 58.3% Ar, while keeping the total pressure constant at 1000 mbar. The time constant of the exponential decay, τ, is determined by the fit (solid line).

volume of the complete system, from the mass flow controllers to the pressure controller, including the reactor and the tubing. Figure 5 shows the pressure evolution in time at two fixed total flows for three different pressure jumps. From these measurements, the volume of the gas system is determined to be 57.4 ± 0.6 ml. Since the intermixing of gas from the reactor into the inlet and outlet was negligible, the only disadvantage of the relatively large volume of the total gas system compared to the reactor is the introduction of a time delay between setting a new gas composition (at constant total pressure) and arrival of the gas in the reactor. At a total flow of 50 ml_n/min and a total pressure of 1000 mbar the time delay is 20 ± 3 s.

The time delay in product gas detection is estimated as the time that CO_2, produced at the sample during a CO oxidation experiment, needs to diffuse through the gas in the reactor to the V-seal®. The diffusion length L is given by

$$L = 2\sqrt{Dt}, \tag{3}$$

where D is the diffusion constant and t is the elapsed time. This is calculated ignoring convection and turbulence, which would mix the gasses in the reactor more efficiently and therefore make the delay in product detection even smaller.

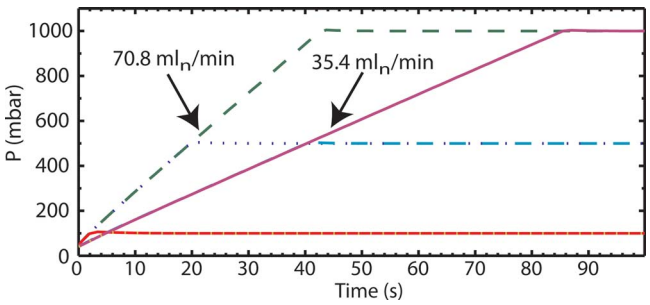

FIG. 5. (Color online) Reactor pressure as a function of time for different flow and pressure settings, starting from an evacuated reactor. The set of curves on the left show the pressure evolution for a total flow of 70.8 ml_n/min of Ar up to a total set pressure on the pressure controller of 1000, 500, and 100 mbar. The set of curves on the right show the evolution for a flow of 35.4 ml_n/min of Ar and a total set pressure of 1000, 500, and 100 mbar.

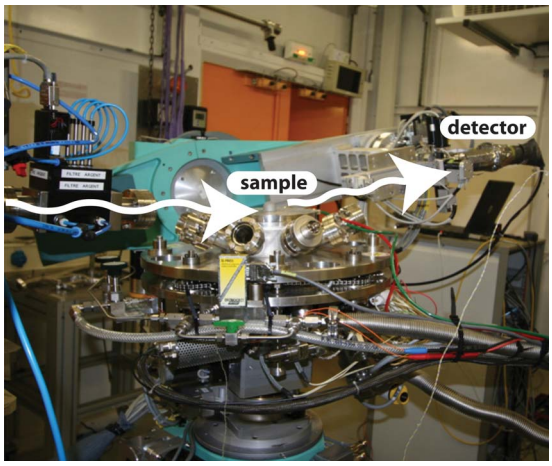

FIG. 6. (Color online) Photograph of the setup installed on the ID03 six-circle diffractometer. The x-ray beam enters from the left and photons scattered from the sample are collected in the detector (white arrows). The setup is shown in the configuration with the reactor closed, such as in Fig. 1(b).

The diffusion constant of CO_2 through air at room temperature is 0.16 cm^2/s.[40] Using above determined time constant for reactor refreshment of 15.8 s, i.e., the average residence time of a molecule in the reactor, we find a diffusion length of 3.1 cm. As the dimensions of the reactor are in the order of 3.2 cm we can be sure that the products will be relatively well mixed, except for the dead volumes in the sample holder, even in the absence of convection and turbulence. Variations in the reaction rate that occur on a timescale faster than the average residence time of a molecule in the reactor are averaged out in the gas detection.

D. First experiment

Figure 6 shows a photograph of the setup mounted on the six-circle diffractometer[24] at the ID03 beamline at the ESRF. During the first test experiment, a Pd(111) sample was mounted in the reactor and cleaned by cycles of 1000 V Ar^+ ion bombardment and annealing up to 1150 K. The sample was first aligned in UHV, i.e., with the Be dome lowered over the sample, but without the reactor closed on the seal. After this alignment, the reactor was fully closed and the alignment of the sample was checked. Figure 7(a) shows that the vertical position of the sample moves down by 27 μm as a result of the force applied on the sample holder support. Also a minor tilt of the crystal of 0.03° was observed. Figure 7(b) shows the variation in vertical position of the sample upon heating. The vertical position of the sample moved up by 28 ± 8 μm, due to thermal expansion of the sample and sample holder. The loss of intensity at 260 °C is caused by a slight accompanying tilt of the crystal by 0.05°. After cooling down, the sample returned to its original, aligned orientation. The alignment is remarkably stable and only modest refinements are necessary when performing experiments over a large temperature range of several hundreds of degrees.

In a later stage a Pd(100) sample was mounted. The surface was cleaned by cycles of 1000 V Ar^+ ion bombardment and annealing up to 1150 K. The surface was subsequently oxidized in a mixture of 50% O_2 and 50 % Ar at a total pressure of 1200 mbar and a temperature of 456 K. A

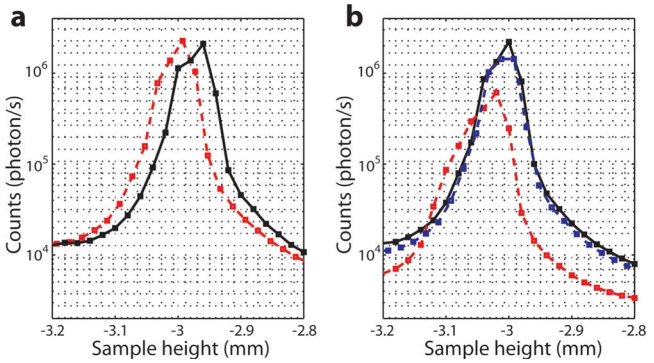

FIG. 7. (Color online) (a) Alignment of the vertical position of the sample surface with the detector at an "anti-Bragg position" of a Pd(111) crystal truncation rod, with the sample in UHV, i.e., with the reactor open (dotted line) and with the sample in the closed reactor (solid line). (b) Alignment of the vertical position of the sample surface on a surface peak at room temperature in UHV, before heating (solid line) and after heating and cool-down (dotted curve overlapping with the solid line) and hot at 260 °C (dotted curve on the left).

bulklike PdO structure, like the one reported in Ref. 41, was found to be present on the surface. The oxide was reduced again by removing O_2 from and adding CO to the mixture. Afterwards a gas mixture was flown through the reactor containing 50% O_2 and variable amounts of Ar and CO. The experiment was performed at a constant temperature of 456 K and a total pressure of 1200 mbar. A typical example of the data that was obtained in this experiment is shown in Fig. 8. A characteristic peak showing the presence of the bulklike PdO is monitored as a function of time while the partial CO pressure in the reactor is varying and while the rate of CO_2 production is measured simultaneously. The presence of a bulklike oxide on the Pd(100) surface is shown to correlate with a high CO_2 production rate. This result is in full agreement with previous results obtained in SXRD and STM.[42,43]

Recently, the new setup has also been successfully used for GISAXS experiments on oxide-supported Pd nanoparticles. The results of these experiments will be published elsewhere.

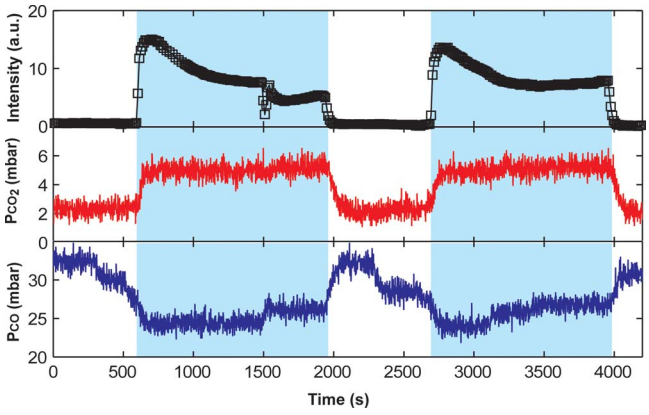

FIG. 8. (Color online) Simultaneous measurement of the intensity of a characteristic PdO diffraction peak (top panel) and the CO_2 production (middle panel) in a CO oxidation experiment on the Pd(100) surface. The CO partial pressure was varied during this experiment (bottom panel), while a compensating amount of inert Ar was mixed in. In this way, the total flow (50 ml_n/min), the partial oxygen pressure (600 mbar), and the total pressure (1200 mbar) in the reactor were kept constant during the experiment. The sample temperature was 456 K. A high value for the CO_2 production rate can be observed simultaneous with the presence of the PdO signal (shaded regions).

E. Additional possibilities

The flexible and open design of the new flow setup allows for the integration of other surface sensitive techniques. The beryllium dome can be replaced by a custom shape made in any material that is transparent to x-rays and suitable as a reactor wall. This opens the possibility to combine the x-ray scattering/diffraction experiments with *in-situ* atomic force microscopy or infrared spectroscopy. The setup, being easily transportable, can in principle be used on other beamlines, specialized on other x-ray techniques, for example EXAFS. Recently the setup has become commercially available from Leiden Probe Microscopy.[44]

[1] G. A. Somorjai, *Introduction to Surface Chemistry and Catalysis* (Wiley, New York, 1993).
[2] G. Ertl, H. Knözinger, and J. Weitkamp, *Handbook of Heterogeneous Catalysis* (Wiley, New York, 1997).
[3] H. Over, Y. D. Kim, A. P. Seitsonen, S. Wendt, E. Lundgren, M. Schmid, P. Varga, A. Morgante, and G. Ertl, Science **287**, 1474 (2000).
[4] N. Lopez, T. V. W. Janssens, B. S. Clausen, Y. Xu, M. Mavrikakis, T. Bligaard, and J. K. Nørskov, J. Catal. **223**, 232 (2004).
[5] A. Stierle, A. M. Molenbroek, MRS Bull. **34**, 12 (2007).
[6] T. W. Hansen, J. B. Wagner, P. L. Hansen, S. Dahl, H. Topsoe, and C. J. H. Jacobsen, Science **294**, 1508 (2001).
[7] P. B. Rasmussen, B. L. M. Hendriksen, H. Zeijlemaker, H. G. Ficke, and J. W. M. Frenken, Rev. Sci. Instrum. **69**, 3879 (1998).
[8] F. Tao, D. Tang, M. Salmeron, and G. A. Somorjai, Rev. Sci. Instrum. **79**, 084101 (2008).
[9] D. F. Ogletree, H. Bluhm, G. Lebedev, C. S. Fadley, Z. Hussain, and M. Salmeron, Rev. Sci. Instrum. **73**, 3872 (2002).
[10] P. Bernard, K. F. Peters, J. Alvarez, and S. Ferrer, Rev. Sci. Instrum. **70**, 1478 (1999).
[11] M.-C. Saint-Lager, A. Bailly, P. Dolle, R. Baudoing-Savois, P. Taunier, S. Garaudée, S. Cuccaro, S. Douillet, O. Geaymond, G. Perroux, O. Tissot, J.-S. Micha, O. Ulrich, and F. Rieutord, Rev. Sci. Instrum. **78**, 083902 (2007).
[12] I. K. Robinson and D. J. Tweet, Rep. Prog. Phys. **55**, 599 (1992).
[13] R. Feidenhans'l, Surf. Sci. Rep. **10**, 105 (1989).
[14] G. Renaud, R. Lazarri, and F. Leroy, Surf. Sci. Rep. **64**, 255 (2009).
[15] M. D. Ackermann, T. M. Pedersen, B. L. M. Hendriksen, O. Robach, S. C. Bobaru, I. Popa, C. Quiros, H. Kim, B. Hammer, S. Ferrer, and J. W. M. Frenken, Phys. Rev. Lett. **95**, 255505 (2005).
[16] J. Gustafson, R. Westerström, A. Mikkelsen, X. Torrelles, O. Balmes, N. Bovet, J. N. Andersen, C. J. Baddeley, and E. Lundgren, Phys. Rev. B **78**, 045423 (2008).
[17] N. Kasper, A. Stierle, P. Nolte, Y. Jin-Phillipp, T. Wagner, D. G. de Oteyza, and H. Dosch, Surf. Sci. **600**, 2860 (2006).
[18] H. Over, O. Balmes, and E. Lundgren, Surf. Sci. **603**, 298 (2009).
[19] K. C. Taylor, Catal. Rev. - Sci. Eng. **35**, 457 (1993).
[20] C. Stegelmann, N. C. Schiødt, C. T. Campbell, and P. Stoltze, J. Catal. **221**, 630 (2004).
[21] R. Pitchai and K. Klier, Catal. Rev. - Sci. Eng. **28**, 13 (1986).
[22] J. Wieckowska, Catal. Today **24**, 405 (1995).
[23] G. P. van der Laan and A. A. C. M. Beenackers, Catal. Rev. - Sci. Eng. **41**, 255 (1999).
[24] HUBER Diffraktionstechnik, www.xhuber.de.
[25] Brush Wellman, www.berylliumproducts.com.
[26] D. E. Nowak, D. R. Blasini, A. M. Vodnick, B. Blank, M. W. Tate, A. Deyhim, D.-M. Smilgies, H. Abruña, S. M. Gruner, and S. P. Baker, Rev. Sci. Instrum. **77**, 113301 (2006).
[27] O. Sakata, Y. Tanaka, A. M. Nikolaenko, and H. Hashizume, J. Synchrotron Radiat. **5**, 1222 (1998).
[28] Jetseal, www.jetseal.com.
[29] Varian S.p.A., www.varianinc.com.
[30] Omicron Technologies, www.omicron-technologies.com.
[31] SPECS GmbH, www.specs.de.

[32] Arun Microelectronics Limited, www.arunmicro.com.
[33] MKS France, www.mksinst.com.
[34] Pfeiffer Vacuum France, www.pfeiffer-vacuum.fr.
[35] Métaux Céramiques Systèmes Engineering, www.mcse.fr.
[36] Saint-Gobain Advanced Ceramics, www.bn.saint-gobain.com.
[37] Bronkhorst, www.bronkhorst.com.
[38] Sigma-Aldrich Chimie S.a.r.l., www.sigmaaldrich.com.
[39] Certified Scientific Software, www.certif.com.
[40] D. R. Lide, *CRC Handbook of Chemistry and Physics* (CRC, Boca Raton, 1994).
[41] A. Stierle, N. Kasper, H. Dosch, E. Lundgren, J. Gustafson, A. Mikkelsen, and J. N. Andersen, J. Chem. Phys. **122**, 044706 (2005).
[42] M. D. Ackermann, Ph.D. thesis, Leiden University, 2007.
[43] B. L. M. Hendriksen, S. C. Bobaru, and J. W. M. Frenken, Surf. Sci. **552**, 229 (2004).
[44] Leiden Probe Microscopy, www.leidenprobemicroscopy.com.